Understanding PDF uncertainty in W boson mass measurements*

Jun Gao(高俊)[1,2†] Dianyu Liu(刘殿宇)[1,2‡] Keping Xie(谢可平)[3§]

[1]NPAC, Shanghai Key Laboratory for Particle Physics and Cosmology, School of Physics and Astronomy, Shanghai Jiao Tong University, Shanghai 200240, China
[2]Key Laboratory for Particle Astrophysics and Cosmology (MOE), Shanghai 200240, China
[3]Pittsburgh Particle Physics, Astrophysics, and Cosmology Center, Department of Physics and Astronomy, University of Pittsburgh, Pittsburgh, PA 15260, USA

Abstract: We study the dependence of the transverse mass distribution of charged leptons and the missing energy on parton distributions (PDFs) adapted to W boson mass measurements at the CDF and ATLAS experiments. We compare the shape variations of the distribution induced by different PDFs and find that the spread of predictions from different PDF sets can be significantly larger than the PDF uncertainty predicted by a specific PDF set. We suggest analyzing the experimental data using up-to-date PDFs to gain a better understanding of the PDF uncertainties in W boson mass measurements. We also perform a series of Lagrange multiplier scans to identify the constraints on the transverse mass distribution imposed by individual data sets in the CT18 global analysis. In the case of the CDF measurement, the distribution is mostly sensitive to d-quark PDFs in the intermediate x region, which are largely constrained by DIS and Drell-Yan data on deuteron targets and Tevatron lepton charge asymmetry data.

Keywords: W-boson mass, PDF uncertainty, CT18

DOI: 10.1088/1674-1137/ac930b

I. INTRODUCTION

Recently, the CDF collaboration released their latest high-precision measurement of the W boson mass using 8.8 fb^{-1} of proton-antiproton collision data recorded at a center-of-mass energy of 1.96 TeV at the Tevatron [1]. The reported result is

$$M_W = 80,433.5 \pm 6.4_{\rm stat} \pm 6.9_{\rm syst}\ {\rm MeV}, \quad (1)$$

which deviates from the standard model electroweak precision fit value $M_W = 80,357 \pm 6$ MeV [2, 3][1)] by seven standard deviations. This new measurement has triggered a number of discussions regarding possible new physics effects (see Refs. [5–91] for examples), standard model effective theory implications [92–95], and evaluations of various theoretical uncertainties [96–100]. Direct measurements have previously been obtained at the 7 TeV LHC by the ATLAS collaboration ($M_W = 80,370 \pm 7_{\rm stat} \pm 18_{\rm syst}$ MeV) [101], the 13 TeV LHC by the LHCb collaboration ($M_W = 80,354 \pm 23_{\rm stat} \pm 22_{\rm syst}$ MeV) [102], and earlier at the Tevatron [103] and LEP [104]. Although there are discussions regarding disagreements between the new CDF measurement and previous values, in this study, we focus on the impact of parton distribution functions (PDFs) on the extracted W boson mass. In the CDF, ATLAS, and LHCb measurements mentioned above, PDF uncertainties of approximately 3.9, 8, and 9 MeV were reported, respectively, which are the dominant theoretical uncertainties in all cases. Note that the three collaborations used very different inputs for the evaluation of the PDF uncertainties. For example, the quoted PDF uncertainty by the CDF is purely based on NNPDF3.1 PDFs [105], despite the impact of different PDFs having been investigated. For the ATLAS measurement, the quoted PDF uncertainty includes those estimated from CT10 PDFs [106] added in quadrature to differences observed using PDFs from several groups. In the LHCb measurement, they took the arithmetic average of the PDF uncertainties predicted by CT18 [107], NNPDF3.1

Received 16 May 2022; Accepted 19 September 2022; Published online 28 September 2022

* JG and DL is supported by the National Natural Science Foundation of China(11875189 and 11835005), as well as the Yangyang Development Fund. KX is supported by the U.S. Department of Energy(DE-SC0007914), U.S. National Science Foundation (PHY-2112829), and in part by the PITT PACC

† E-mail: jung49@sjtu.edu.cn
‡ E-mail: dianyu.liu@sjtu.edu.cn
§ E-mail: xiekeping@pitt.edu

1) The HEPfit group gives a consistent global fit as $M_W = 80,354.5 \pm 5.7$ MeV [4].

[105], and MSHT20 [108] PDFs. The LHCb also reported a spread of the central values of the extracted W boson mass from the three PDFs, which was as large as 11 MeV and was not counted in the final uncertainty.

The method in which PDFs change the modeling of the kinematics of decayed leptons in W boson production can be understood as described below. The fully differential cross sections of the decayed leptons can be written as

$$\frac{\mathrm{d}^2\sigma}{\mathrm{d}p_1\mathrm{d}p_2} = \left[\frac{\mathrm{d}\sigma(m)}{\mathrm{d}m}\right]\left[\frac{\mathrm{d}\sigma(y)}{\mathrm{d}y}\right]\left[\frac{\mathrm{d}^2\sigma(p_T,y)}{\mathrm{d}p_T\mathrm{d}y}\left(\frac{\mathrm{d}\sigma(y)}{\mathrm{d}y}\right)^{-1}\right] \times\left[(1+\cos^2\theta)+\sum_{i=0}^{7}A_i(p_T,y)P_i(\cos\theta,\phi)\right], \quad (2)$$

where $p_{1(2)}$ is the lepton (anti-lepton) momentum; m, p_T, and y are the invariant mass, transverse momentum, and rapidity of the dilepton system, respectively; θ and ϕ are the polar angle and azimuth of p_1 in the rest frame of the dilepton system, respectively; A_i are angular coefficients; and P_i are spherical harmonics. The cross sections are factorized in this way because each component on the right-hand side of Eq. (2) is modeled or corrected separately using different MC programs during experimental analyses [101]. The impact of PDF uncertainties on each individual component can be understood. For example, the effects of PDF variations on the angular coefficients and invariant mass distribution are found to be small in W boson mass measurements. Most of the PDF uncertainties in the extracted W boson mass originate from the impact on the rapidity distribution of the W boson. PDF variations, especially those from the gluon PDF, will also affect the W boson transverse momentum distribution at large-p_T. A complication of the p_T distribution is that the CDF analysis used a data-driven method to model the measured transverse momentum distribution of the Z boson, which was then applied to the W boson to reduce theoretical uncertainties. Thus, for the component of the p_T distribution, only the theoretical uncertainties on the ratio of the p_T spectrum of the W boson and Z boson should, in principle, be included.

In this study, we perform a comprehensive comparison of the kinematic distribution of decayed leptons using a variety of up-to-date PDFs, focusing on the CDF and ATLAS measurements. Previous studies have also been conducted on the PDF uncertainties in W boson mass measurements [109– 113]. We reveal variations in the shape of the transverse mass distribution from different PDF groups and different generations within the same group and estimate the possible shift in the extracted W boson mass. Furthermore, using Lagrange multiplier (LM) scans, we evaluate the constraints on the prescribed distribution as imposed by different experimental data sets in the CT18 global analysis of PDFs. Other theoretical uncertainties, including factorization and renormalization scales, the strong coupling constant, and the W-boson decay width, are also examined in the CDF scenario. Note that we include the full PDF uncertainty in the modeling of the p_T of the W boson for results calculated at next-to-leading order (NLO) in QCD, unlike the prescription used in the experimental analyses mentioned above. However, we also show results calculated at leading order (LO) for comparison, where the PDF uncertainty in the modeling of p_T is completely removed. In this study, we aim to understand the PDF uncertainties in the W boson mass measurements, especially using the most up-to-date PDFs, rather than reproducing the exact PDF dependence in actual experimental analyses.

The rest of this paper is organized as follows. In Sec. II, we present the results of the kinematic distribution and extracted W boson mass. In Sec. III, we show the results of PDF sensitivities and our understanding of constraints within the CT18 analysis using the LM method. Finally, our summary and conclusions are presented in Sec. IV.

II. PDF DEPENDENCE OF THE KINEMATIC DISTRIBUTION

In this section, we show the dependence of the transverse mass distribution of charged leptons and the missing energy on PDFs and the change in the W boson mass under the setups of both the CDF and 7 TeV ATLAS measurements. Note that in both the CDF and ATLAS measurements, the PDF uncertainties are fully correlated to the results using three different kinematic variables and are almost the same. We calculate the mean value of the transverse mass to quantify the impact of different PDFs on the shape of the kinematic distribution. We further propose a simplified prescription to identify the PDF impact on the extracted W boson mass and validate it against a method with a log-likelihood χ^2 fit.

A. CDF measurement

The event selection criterion follows that of the CDF Run II measurement [1]

$$30 < p_T^{\ell,\nu} < 55\ \mathrm{GeV},\ u_T < 15\ \mathrm{GeV},\ 60 < M_T < 100\ \mathrm{GeV}, \quad (3)$$

where $u_T = |\vec{p}_T^{\,\ell} + \vec{p}_T^{\,\nu}|$ is the transverse momentum of the W boson. The transverse mass of the W boson is defined as $M_T = \sqrt{2(p_T^{\ell}p_T^{\nu} - \vec{p}_T^{\,\ell}\cdot\vec{p}_T^{\,\nu})}$. The charged lepton is also required to be in the central pseudo-rapidity region

$$|\eta| < 1. \quad (4)$$

The transverse mass distribution of the charged lepton

and missing energy are calculated using the program MCFM-6.8 [114, 115] with the above selections at either LO or NLO in QCD and with the APPLgrid interface [116] for fast interpolations with arbitrary PDFs. We do not consider QCD resummation effects on the transverse momentum of the W boson because they should be less pronounced for the M_T distribution and because of the constraints of repeating calculations for a large number of PDF sets with sufficient numerical accuracy. For the same reasons, we do not included next-to-next-to-leading order (NNLO) QCD corrections, which we expect will not significantly change our conclusions on PDF dependence. The factorization and renormalization scales are chosen to be the invariant mass of the charged lepton and neutrino pair, $\mu_F = \mu_R = M_{\ell\nu}$. We apply Gaussian smearing on the distributions from theoretical calculations, assuming a detector resolution of 7% for M_T, which is consistent with the resolution on hadronic recoils reported in the CDF paper [1]. We check that the prescribed smearing effects can effectively reproduce the shape of the experimental distribution, especially in the region close to the peak. In principle, one can apply more sophisticated detector effects with energy-dependent resolution for individual objects. We do not expect a large difference, especially because we are focusing on the mean value of the kinematic distribution, which is less affected by smearing effects.

In Fig. 1, we show the predicted normalized M_T distribution at LO and NLO for several choices of PDFs and different values of the W boson mass. From top to bottom, the figure shows the normalized distribution, and the absolute and relative variations compared to a common reference calculated with the central set of NNPDF3.1 NNLO PDFs [105]. The red dashed lines represent the variation due to a W boson mass change of $\pm$10 MeV, and the gray band indicates the PDF uncertainties at a 68% confidence level (C.L.) for NNPDF3.1. The different PDFs under consideration include CTEQ6M [117] NLO PDFs, and CT18 [107], MMHT14 [118], and NNPDF4.0 [119] NNLO PDFs. PDF uncertainties are calculated using the respective prescription, as summarized in Ref. [120]. In the lower panel of each figure, the variations are divided by the statistical uncertainty in each bin to show the significance. We choose a bin width of 0.5 GeV and normalize the total number of events to the number of muon events in the CDF measurement for the calculation of the statistical uncertainty.

Several interesting observations were made. First, we find that there can be a significant difference in the PDF dependence between LO and NLO, whereas the W boson mass dependence is significantly more stable. This may be due to the gluon contributions at NLO, which boost the W boson in the transverse direction. The gluon PDF is considerably different in CTEQ6M compared with recent NNLO PDFs, which leads to the large differences observed in the NLO plot. This can be traced back to the fact that the CTEQ6M analysis uses a zero-mass scheme for heavy-quark effects in DIS rather than variable flavor number schemes [121]. However, we stress that in the experimental analyses, because data on the Z boson p_T spectrum are used to model the W boson p_T spectrum, only PDF uncertainties in the ratio of the W and Z boson p_T spectra should be considered for p_T modeling, unlike the rapidity distribution of the W boson. We focus on the

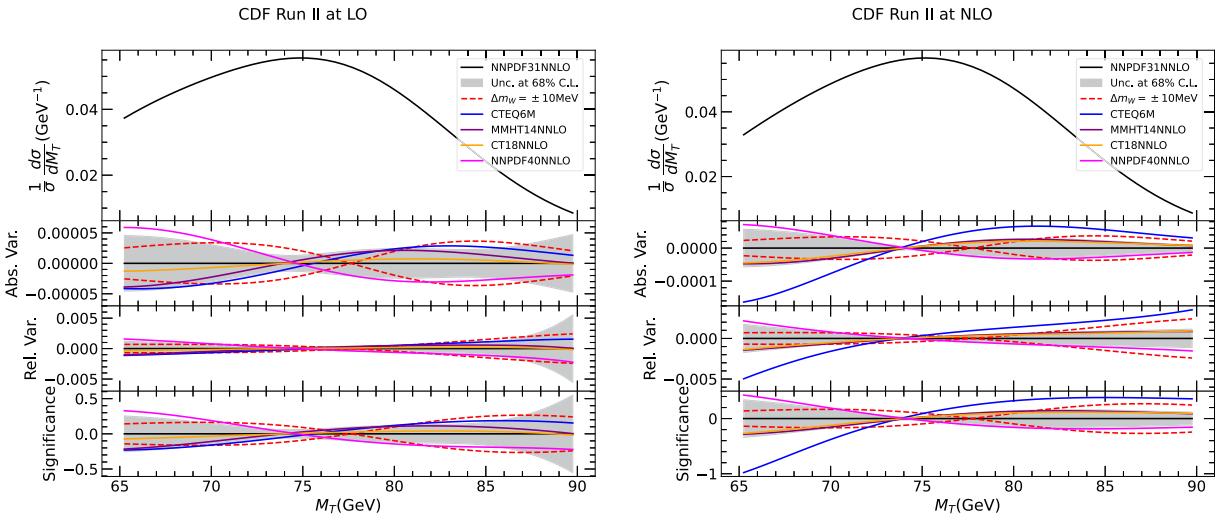

Fig. 1. (color online) Transverse mass distribution of the charged lepton and missing energy in the scenario of the CDF measurement calculated at LO and NLO with various PDFs and different values of the W boson mass (increased or decreased by 10 MeV). From top to bottom are the normalized distribution, and absolute and relative changes with respect to a common reference of the prediction obtained using NNPDF3.1 NNLO PDFs and the nominal W boson mass. The lowest panel shows the changes normalized to the experimental statistical uncertainties.

predictions calculated at NLO unless specified. We find that the PDF uncertainty of NNPDF3.1 tends to be similar in size compared to the impact of varying M_W by 5 MeV, and CT18 and MMHT14 prefer a harder spectrum within the uncertainty of NNPDF3.1. This is in qualitative agreement with the CDF results regarding PDF uncertainty and dependence. The PDF variations of NNPDF4.0 are opposite to those of CT18 and MMHT14 and are close to the boundaries of the uncertainty of NNPDF3.1.

We construct a principle variable to describe the impact of different PDFs on the shape of the M_T distribution. This is the mean value of M_T within a select window of [70, 90] GeV, denoted as $\langle M_T \rangle$. A similar shape parameter proposed by Kotwal in Ref. [122] plays the same role. We choose this window in accordance with the CDF analysis because kinematic bins in this range exhibit the largest significance when varying M_W. In Fig. 2, we plot various predictions on $\langle M_T \rangle$ at NLO and LO, including PDF uncertainties at a 68% C.L., by normalizing to a common reference of the central prediction of NNPDF3.1. Here, we further include the CT10 [106], CT14 [123], CT18Z [107], MSTW2008 [124], NNPDF2.3 [125], MSHT20 [108], ABMP16 [126], HERAPDF2.0 [127], ATLASepWZVjet20 [128], and CJ15 [129] PDFs for comparison. We also present the range of $\langle M_T \rangle$ when varying M_W by ±5 MeV. In general, the predictions from all of the NNLO PDFs agree within uncertainties. The spread of their central values at NLO can be as large as the shift in M_W of 15 MeV if those from HERA and ATLAS PDFs are not considered. This number is smaller at approximately 10 MeV for LO predictions. The size of the PDF uncertainties is consistent among NNLO PDFs, with CT18 being one of the largest at approximately twice that of NNPDF3.1. Moreover, when comparing the results from up-to-date PDFs with previous values of the same PDF group, we find that the PDF uncertainties can even increase in many cases. NLO PDFs predict larger $\langle M_T \rangle$ in general compared to NNLO

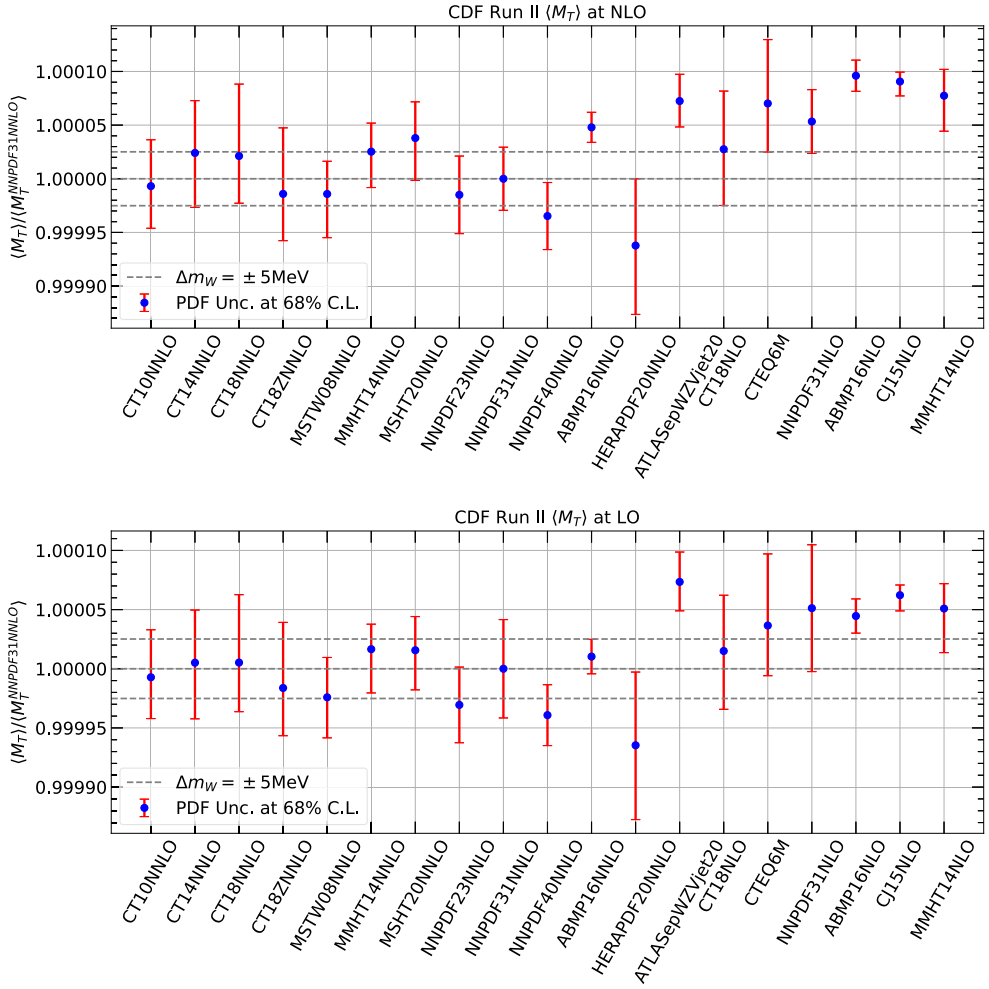

Fig. 2. (color online) Mean transverse mass of the charged lepton and missing energy in the scenario of the CDF measurement calculated at NLO or LO with various PDFs, normalized to the central prediction of NNPDF3.1 NNLO PDFs. The error bars represent PDF uncertainties at a 68% C.L., and the horizontal lines indicate variations induced by a W boson mass change of ±5 MeV.

PDFs.

Figure 2 shows a simplified prescription using $\langle M_T \rangle$ to quantify the shift in the extracted W boson mass when using different PDFs and the associated uncertainties. Ideally, one can consider the shift in M_W to compensate for the change in $\langle M_T \rangle$ induced by the variation of PDFs. We summarize the estimated shifts in the extracted M_W with respect to NNPDF3.1 and associated PDF uncertainties in Table 1 and compare them to the results in the CDF analysis when available. Using the $\langle M_T \rangle$ prescription NNPDF3.1 gives a PDF uncertainty of 5.7 MeV for the extracted W boson mass at NLO; in contrast, a value of 3.9 MeV is obtained from the CDF analysis. The envelope of extracted M_W values from the central sets of NNPDF3.1, CT18, and MMHT14 is approximately 5.0 MeV, whereas the envelope is 4.2 MeV from the CDF analysis. Thus, the simplified prescription is in reasonable agreement with the dedicated simulation in the CDF analysis. However, using the $\langle M_T \rangle$ prescription, we find a δM_W value of -14 MeV when comparing CTEQ6M with NNPDF3.1, whereas this value is -3.3 MeV from the CDF analysis. The shift is reduced to -7.3 MeV when using LO calculations of $\langle M_T \rangle$. Another interesting observation is that for the most recent NNLO PDFs, namely CT18, MMHT20, and NNPDF4.0, the envelope of extracted M_W from their central sets is enlarged to 15(11) MeV at NLO(LO), which is larger than that of the previous generation. This further motivates the analysis of W boson mass data using up-to-date PDFs.

The CDF analysis dependence of the extracted M_W on PDFs is studied via fitting to pseudo experiments. We perform similar studies and use the predictions of NNPDF3.1 NNLO PDFs as pseudo-data. We calculate χ^2 as a function of M_W to use predictions from various PDFs, considering only statistical uncertainties because they are dominant over experimental systematic uncertainties. Then, we can estimate the shift in the extracted M_W as well as the statistical and PDF uncertainties included in Table 1 for comparison. We can see that the χ^2 fit indicates a statistical uncertainty on the extracted M_W of 8.0 MeV, which is consistent with the value of 9.2 MeV from the CDF measurement on the muon channel alone. The χ^2 fit shows very good agreement for the projected shift in the extracted M_W for different PDFs with respect to the previous simplified prescription using $\langle M_T \rangle$. The estimated PDF uncertainties are slightly smaller than previous values because the χ^2 fit does account for the higher moments of the kinematic distribution.

Besides the PDF dependence, we also explore other theoretical uncertainties, including the factorization and renormalization scales, strong coupling constant, and W-boson decay width, based on a χ^2 fit of the transverse mass distribution at NLO with CT18 NNLO PDFs. The results are summarized in Table 2 and discussed in sequence as follows:

- The scale uncertainty is estimated with the envelope of seven-point variation,

$$(\mu_F,\mu_R) = \{(1/2,1/2),(1/2,1),(1,1/2),(1,1),(1,2),(2,1),(2,2)\} M_{\ell\nu}. \quad (5)$$

It is found that maximal shifts in M_W are -3.0 and +3.1 MeV. However, we expect the impact of scale variations to be largely reduced once higher order corrections are included.

- The strong coupling constant can impact M_W extraction in two ways. First, starting from NLO, high-order corrections to W boson production are directly involved in the QCD interaction. Second, different choices of strong coupling in the QCD global analysis will lead to different PDFs, with the impact propagating to M_W extraction. We quantify the dependence by varying α_s between 0.116 and 0.120 along with consistent PDF variations. This changes the extracted M_W by -1.3 and +1.2 MeV, respectively.

- To date, the most precise measurements of the W-boson decay width Γ_W have originated from the LEP [104] and Tevatron [130], which gave a combined result of

Table 1. Estimated shifts and PDF uncertainties at a 68% C.L. in the extracted W boson mass of the CDF scenario for various PDF sets with respect to a common reference using an NNPDF3.1 NNLO central PDF. The results are presented using the simplified prescription and compared with those from a χ^2 fit as well as results reported in the CDF analysis. In the case of the χ^2 fit, we also show the expected experimental statistical error of the extracted W boson mass compared to the actual value in the CDF analysis.

δM_W in MeV	sta.	NNPDF3.1	CT18	MMHT14	NNPDF4.0	MSHT20	CTEQ6M
$\langle M_T \rangle$(LO)	–	$0^{+8.3}_{-8.3}$	$-1.0^{+8.3}_{-11.4}$	$-3.3^{+7.4}_{-4.2}$	$+7.8^{+5.1}_{-5.1}$	$-3.1^{+6.7}_{-5.7}$	$-7.3^{+8.4}_{-12.0}$
χ^2 fit (LO)	8.0	$0^{+7.6}_{-7.6}$	$-1.0^{+5.4}_{-8.6}$	$-3.3^{+6.1}_{-3.0}$	$+8.0^{+3.7}_{-3.7}$	$-3.0^{+5.0}_{-4.0}$	$-7.3^{+5.6}_{-9.3}$
$\langle M_T \rangle$(NLO)	–	$0^{+5.9}_{-5.9}$	$-4.2^{+8.8}_{-13.3}$	$-5.0^{+6.7}_{-5.3}$	$+6.9^{+6.2}_{-6.2}$	$-7.6^{+7.9}_{-6.7}$	$-14.0^{+9.0}_{-11.9}$
χ^2 fit (NLO)	8.0	$0^{+4.2}_{-4.2}$	$-4.3^{+5.4}_{-10.1}$	$-5.1^{+4.8}_{-3.4}$	$+7.1^{+4.5}_{-4.5}$	$-7.8^{+5.7}_{-4.5}$	$-14.6^{+5.8}_{-5.4}$
CDF	9.2	$0^{+3.9}_{-3.9}$	–	–	–	–	-3.3

Table 2. Dependence of M_W extraction on the factorization and renormalization scales, strong coupling constant, and W-boson decay width in the CDF scenario.

Variation	$\mu_{F,R}$ (7-point)	$\alpha_s = 0.118 \pm 0.002$	$\Gamma_W = 2,085 \pm 42$MeV
χ^2 fit (NLO)	$0^{+3.1}_{-3.0}$	$0^{+1.2}_{-1.3}$	$0^{+7.1}_{-6.8}$

$\Gamma_W = 2,085 \pm 42$ MeV [3]. In experimental analyses, the CDF collaboration adopted the electroweak global fitting value of $2,089.5 \pm 0.6$ MeV [3] and found that the uncertainty induced by the input width was negligible. However, if the W-boson width is allowed to vary by 42 MeV, which is the error from direct measurements, we find that the normalized M_T distribution can deviate significantly (up to 2% at $M_T \sim 90$ GeV). As a result, the extracted M_W value can shift by -6.8 (+7.1) MeV, comparable to the full uncertainty on the CDF measurement. This suggests that a simultaneous fit of the W-boson mass and width is possible and may result in comparable precision on the width measurement.

B. ATLAS measurement

We repeat a similar exercise for the 7 TeV ATLAS measurement. The event selection criterion follows [101]

$$p_T^{\ell,\nu} > 30 \text{ GeV}, \; u_T < 30 \text{ GeV}, \; M_T > 60 \text{ GeV}. \tag{6}$$

The pseudo-rapidity of the charged lepton is required to satisfy

$$|\eta| < 2.4. \tag{7}$$

We use the same theoretical setups as in the calculations for the CDF scenario; however, separate calculations must be performed for W^+ and W^- production. We assume a detector resolution of 10% for M_T to effectively reproduce the shape of the measured distribution.

In Fig. 3, we show the predictions of the normalized M_T distribution at NLO for several choices of PDFs and different values of the W boson mass for both W^+ and W^- production. We find that the PDF variations are approximately twice those shown in Fig. 1 for the CDF scenario, whereas the dependence on the W boson mass is similar in size. The PDFs clearly alter W^+ and W^- production in different ways, evident by the fact that the NNPDF4.0 central predictions lie on opposite sides of CT10 for W^+ and W^-. The PDF uncertainties of CT10 are larger for W^- production than W^+ production, possibly because of the relatively larger contributions from the strange quark in the former case. The significance in the lowest panel is calculated assuming a total number of events equal to that from the ATLAS measurement of the muon channel and a bin width of 0.5 GeV.

Similar to the CDF case, Fig. 4 shows the mean transverse mass within a window of [65, 100] GeV for W^+ and W^- production with various choices of PDFs. All predictions are normalized to the central prediction from CT10 NNLO PDFs, including those with a W boson mass change of ±5 MeV. We find a wider spread of predictions from different PDFs and larger PDF uncertainties compared to Fig. 2, which is consistent with observations in the normalized distributions. We can again use the simplified prescription to estimate the expected shift in the extracted W boson mass and the associated PDF un-

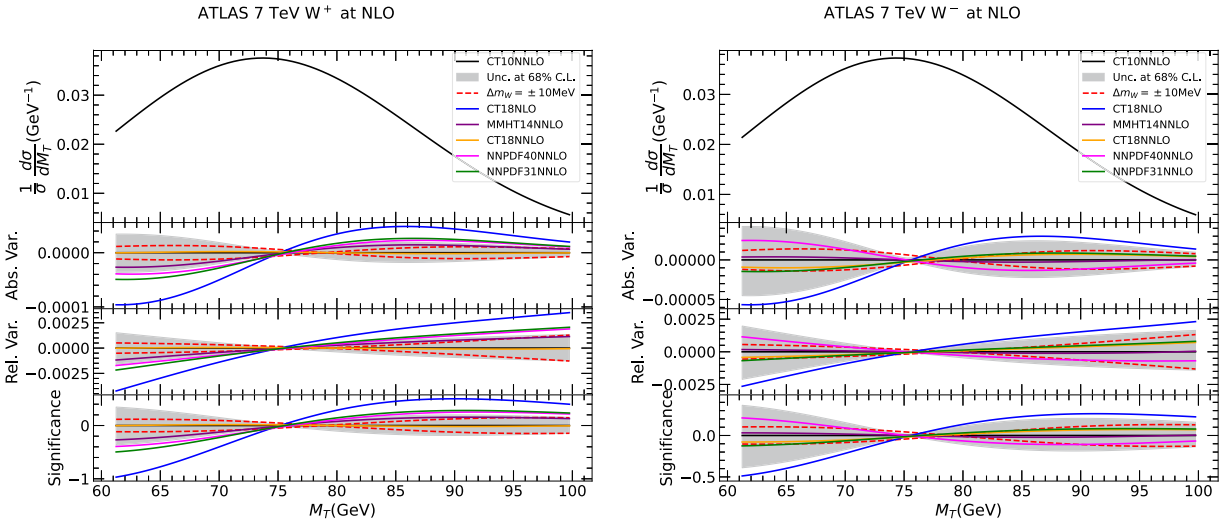

Fig. 3. (color online) Transverse mass distribution of the charged lepton and missing energy in the scenario of the ATLAS measurement for W^+ and W^- with various PDFs and different values of the W boson mass (increased or decreased by 10 MeV) calculated at NLO. From top to bottom are the normalized distribution, and absolute and relative changes with respect to a common reference of the prediction obtained with CT10 NNLO PDFs and the nominal W boson mass. The lowest panel shows the changes normalized to the experimental statistical uncertainties.

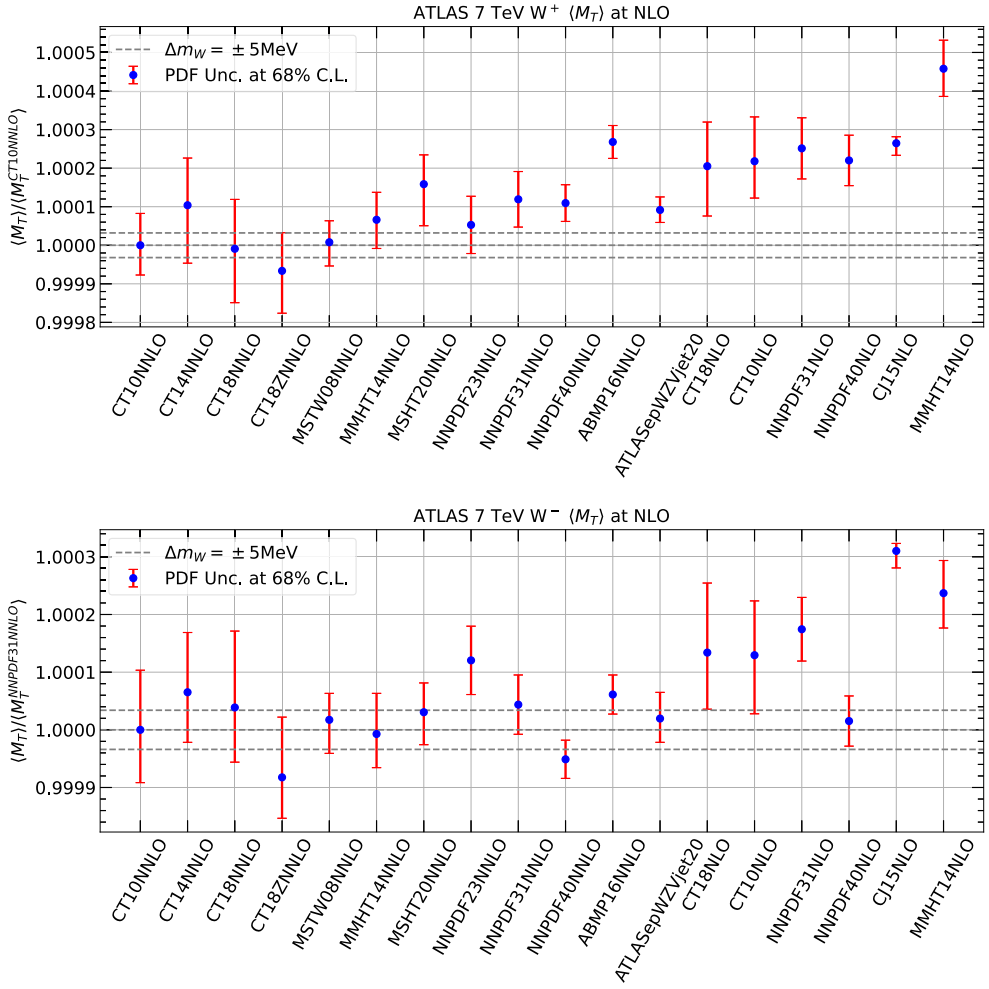

Fig. 4. (color online) Mean transverse mass of the charged lepton and missing energy in the scenario of ATLAS measurement calculated at NLO with various PDFs, normalized to the central prediction of CT10 NNLO PDFs, for W^+ and W^- production. The error bars represent PDF uncertainties at a 68% C.L., and the horizontal lines indicate variations induced by a W boson mass change of ±5 MeV.

certainties, which are summarized in Table 3. For example, we estimate a PDF uncertainty of approximately 13 and 14 MeV with CT10 NNLO PDFs for W^+ and W^-, respectively, whereas ATLAS reported 15 and 14 MeV, respectively. We also note that the central sets of both NNPDF4.0 and MSHT20 prefer a downward shift in M_W of almost 20 MeV for W^+ production compared with those of CT10. These shifts are generally smaller for W^- production. We take an unweighted average of the W^+ and W^- results on $\langle M_T \rangle$ and show the shift in the extracted W boson mass in Table 3, denoted as $W^\pm$. The combinations reveal less spread of the expected shift in M_W, and the PDF uncertainties are generally reduced. The PDF uncertainty in the W boson mass for $W^\pm$ decreases slightly to 11 MeV for CT10 NNLO PDFs. In the ATLAS analysis, the combined $W^\pm$ results exhibit a PDF uncertainty of approximately 7 MeV, which is largely reduced compared to those of W^+ and W^- alone owing to the anti-correlations of PDF dependence in the two. We observe a similar pattern for CT10 when using LO calculations instead of NLO, that is, by excluding PDF uncertainties due to the modeling of the W boson p_T. The corresponding results are also summarized in Table 3.

III. LAGRANGE MULTIPLIER SCAN

In this section, we study the PDF uncertainties of the W boson mass measurements in the context of the CT18 global analysis. We focus on the observable of the mean transverse mass, which is strongly anti-correlated with the extracted W boson mass, as previously shown. We first reveal correlations between $\langle M_T \rangle$ and PDFs of different flavors and momentum fractions x and those of $\langle M_T \rangle$ in different measurements. This is followed by a series of LM scans to understand the constraints imposed by individual data sets in the CT18 global analysis.

A. PDF induced correlations

We study the PDF-induced correlations of the observ-

Table 3. Estimated shifts and PDF uncertainties at a 68% C.L. of the extracted W boson mass in the ATLAS scenario for various PDF sets with respect to a common reference using the CT10 NNLO central PDF. We show the results with the simplified prescription and calculations at NLO and LO and compare them to the values from the ATLAS analysis.

δM_W in MeV	CT10	CT18	MMHT14	NNPDF4.0	CT14	MSHT20
W^+ $\langle M_T\rangle$ (NLO)	$0^{+12.1}_{-12.9}$	$+1.4^{+21.8}_{-20.0}$	$-10.3^{+11.6}_{-11.1}$	$-17.1^{+7.4}_{-7.4}$	$-16.2^{+23.5}_{-19.1}$	$-24.8^{+16.8}_{-11.9}$
W^- $\langle M_T\rangle$ (NLO)	$0^{+13.5}_{-15.2}$	$-5.7^{+14.0}_{-19.5}$	$+1.1^{+8.6}_{-10.3}$	$+7.5^{+4.9}_{-4.9}$	$-9.6^{+12.8}_{-15.3}$	$-4.5^{+8.3}_{-7.5}$
$W^\pm$ $\langle M_T\rangle$ (NLO)	$0^{+9.8}_{-11.4}$	$-2.3^{+14.4}_{-16.8}$	$-4.5^{+8.2}_{-8.5}$	$-4.4^{+4.6}_{-4.6}$	$-12.8^{+16.6}_{-15.1}$	$-14.3^{+10.9}_{-8.0}$
W^+ $\langle M_T\rangle$ (LO)	$0^{+10.8}_{-11.4}$	$-6.5^{+14.1}_{-10.0}$	$-5.7^{+8.1}_{-7.1}$	$-14.1^{+5.8}_{-5.8}$	$-4.1^{+15.0}_{-12.9}$	$-14.4^{+10.2}_{-7.3}$
W^- $\langle M_T\rangle$ (LO)	$0^{+8.9}_{-11.4}$	$-7.2^{+10.1}_{-12.5}$	$+3.1^{+8.3}_{-9.9}$	$+3.5^{+4.5}_{-4.5}$	$-7.0^{+6.2}_{-8.9}$	$+2.1^{+6.3}_{-4.9}$
$W^\pm$ $\langle M_T\rangle$ (LO)	$0^{+5.2}_{-7.0}$	$-0.6^{+7.6}_{-7.4}$	$-1.2^{+5.3}_{-5.9}$	$-5.0^{+3.0}_{-3.0}$	$-5.6^{+8.0}_{-8.4}$	$-5.9^{+5.9}_{-4.2}$
W^+ ATLAS	$0^{+14.9}_{-14.9}$	–	–	–	–	–
W^- ATLAS	$0^{+14.2}_{-14.2}$	–	–	–	–	–
$W^\pm$ ATLAS	$0^{+7.4}_{-7.4}$	–	–	–	–	–

ables proposed in the previous section, namely, the mean transverse mass of the charged lepton and missing energy in the CDF and ATLAS measurements. The correlations are calculated using CT18 NNLO PDFs with the transverse mass distributions at NLO by default. In the Hessian approach, the correlations between two observables, X and Y, can be estimated [131]:

$$\cos(\Delta\varphi) = \frac{\sum_{i=1}^{N_{\rm eig}}\left(X_i^+ - X_i^-\right)\left(Y_i^+ - Y_i^-\right)}{\sqrt{\sum_{i=1}^{N_{\rm eig}}\left[X_i^+ - X_i^-\right]^2}\sqrt{\sum_{i=1}^{N_{\rm eig}}\left[Y_i^+ - Y_i^-\right]^2}}, \quad (8)$$

where $\Delta\varphi$ is the correlation angle, and $X_i^\pm$ ($Y_i^\pm$) represent the values of X (Y), with the error on the PDF of the Hessian set in the positive and negative directions of the $i_{\rm th}$ eigenvector in $N_{\rm eig}$-dimensional PDF parameter space. In addition, the error ellipse for X and Y, which is determined using CT18 NNLO PDFs at a 68% C.L., can be found using the following parametric equations [131]:

$$\begin{cases} X(\theta) = \dfrac{1}{2\times 1.645}\sqrt{\sum_{i=1}^{N_{\rm eig}}\left[X_i^+ - X_i^-\right]^2}\cos\theta, \\ Y(\theta) = \dfrac{1}{2\times 1.645}\sqrt{\sum_{i=1}^{N_{\rm eig}}\left[Y_i^+ - Y_i^-\right]^2}\cos(\theta+\Delta\varphi), \\ (0 \le \theta < 2\pi). \end{cases} \quad (9)$$

In Fig. 5, we plot the correlations between $\langle M_T\rangle$ and PDFs of various flavors at different x values and with $Q = 100$ GeV. In the scenario of CDF measurement, $\langle M_T\rangle$ is anti-correlated with a d-quark at $x \sim 0.01$ because this corresponds to a W boson produced in large rapidity regions, where the decayed lepton has a smaller average p_T, as explained later in Sec. III.C. For the same reason, $\langle M_T\rangle$ in the case of W^+ production at 7 TeV ATLAS is anti-correlated with the $\bar{d}$ quark, but now at $x \sim 0.002$. In the ATLAS W^- production at 7 TeV, various sea quarks exhibit moderate anti-correlations, including the strange quark. For the average $\langle M_T\rangle$ of W^+ and W^- production at ATLAS, the correlations exhibit an average pattern of the two.

We plot a 68% C.L. relative error ellipse for each pair of observables in Fig. 6 at both NLO and LO. As shown, the PDF uncertainty of $\langle M_T\rangle$ at ATLAS is approximately twice that at the CDF, which is consistent with the results shown in an earlier section; the two are also largely uncorrelated. This suggests that the PDF uncertainty in the extracted M_W can be further reduced by combining the CDF and ATLAS measurements. However, the PDF uncertainties of $\langle M_T\rangle$ for W^+ and W^- production at ATLAS are only partially correlated at NLO and anti-correlated at LO. Combining the $\langle M_T\rangle$ of W^+ and W^- will reduce the PDF uncertainty, especially at LO, as it is evident from Table 3.

B. Constraints on CT18

LM scanning is a robust method of estimating PDF uncertainties, which was originally developed in Refs. [132, 133]. In this method, PDF uncertainties of an observable can be determined from the profiled χ^2 as a function of the observable without relying on any assumptions about the specific behavior of χ^2 around the global minimum. However, the LM method requires a detailed scan of the PDF parameter space for every observable studied, which is usually time-consuming. To overcome this drawback, we take advantage of neural networks (NNs) and machine learning techniques to model the profiles of χ^2 and $\langle M_T\rangle$ for multi-dimensional parameter space, which work beyond quadratic approximations and ensure efficient scans of the entire parameter space. The setup of the NNs and further details can be found in Ref. [134].

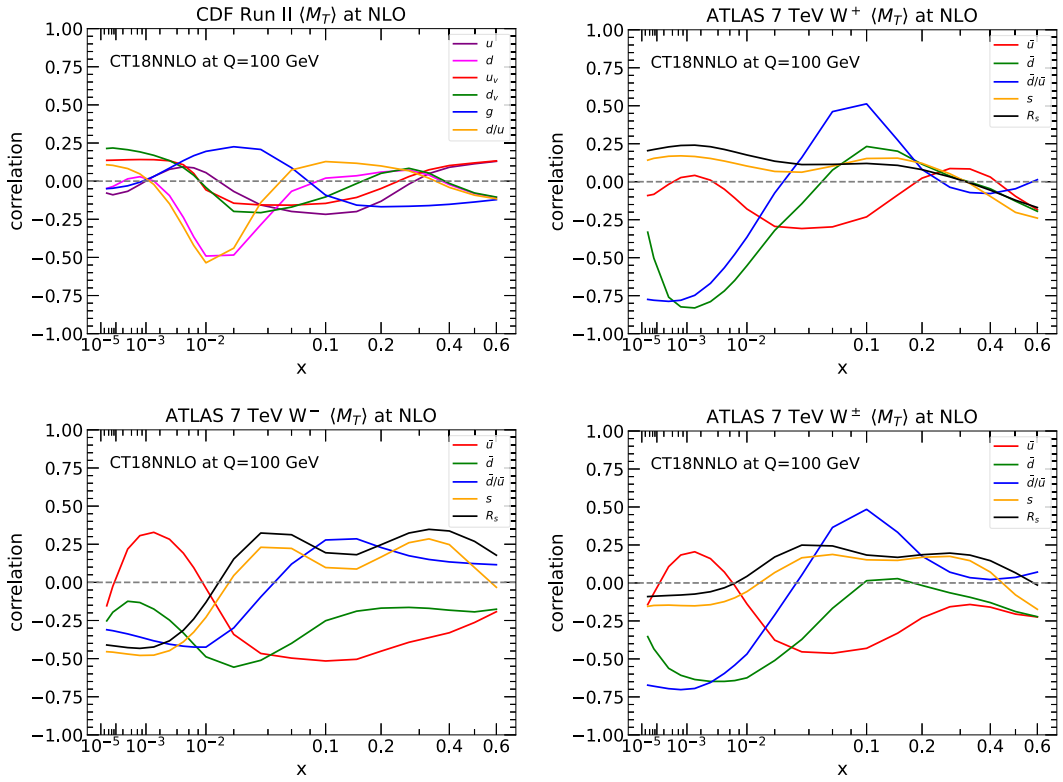

Fig. 5. (color online) Correlations between ⟨M_T⟩ calculated at NLO and PDFs of different flavors as a function of x in the scenarios of CDF and ATLAS measurements of W^+, W^-, and their combination using CT18 NNLO PDFs.

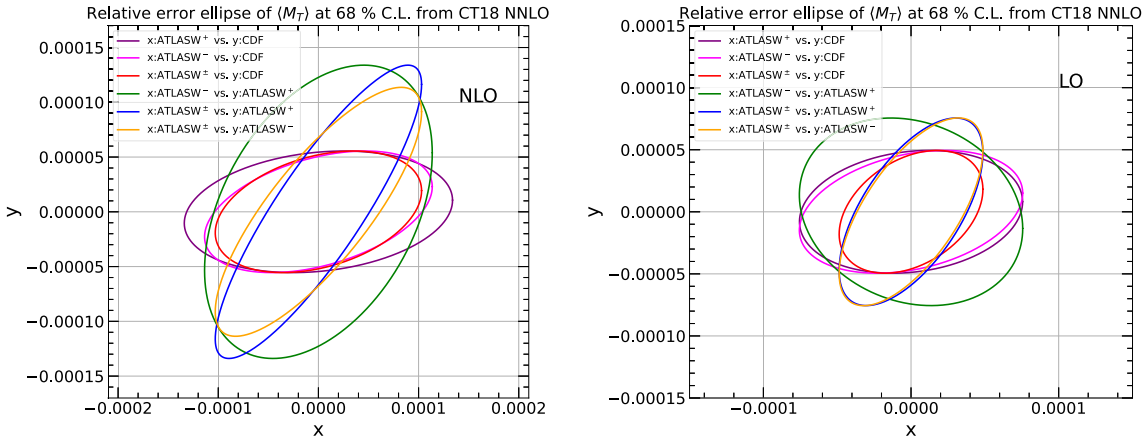

Fig. 6. (color online) Relative error ellipse at a 68% C.L. for each pair of ⟨M_T⟩ in the scenarios of the CDF and ATLAS measurements of W^+, W^-, and their combination, calculated at NLO and LO using CT18 NNLO PDFs.

In Fig. 7, we show the results of LM scans on ⟨M_T⟩ based on the aforementioned NNs. The black and red solid lines indicate $\Delta\chi^2$ and $\Delta\chi^2 + P$, respectively, where P, known as a Tier-2 penalty [120, 123], is introduced to ensure that the tolerance is reached as soon as any data set shows disagreement at a 90% C.L. The PDF uncertainty of ⟨M_T⟩ at a 90% C.L. can be determined by requiring $\Delta\chi^2 + P = 100$, following the CT18 analysis. The dotted and dashed lines represent the contributions to $\Delta\chi^2$ from individual data sets. The blue and green vertical dot-dashed lines indicate the uncertainties at a 90% C.L. determined using the LM and Hessian methods [124, 135] from the published CT18 NNLO PDFs, respectively. The profiles of the total $\Delta\chi^2$ and individual $\Delta\chi^2$ exhibit an almost quadratic dependence on the variable in the vicinity of the global minimum. In the case of the CDF measurement, in the left panel, NMC deuteron to proton ratio data along with D0 Run II charge asymmetry data and E866 Drell-Yan deuteron to proton ratio data give the dominant constraints. The penalty term contributes largely to

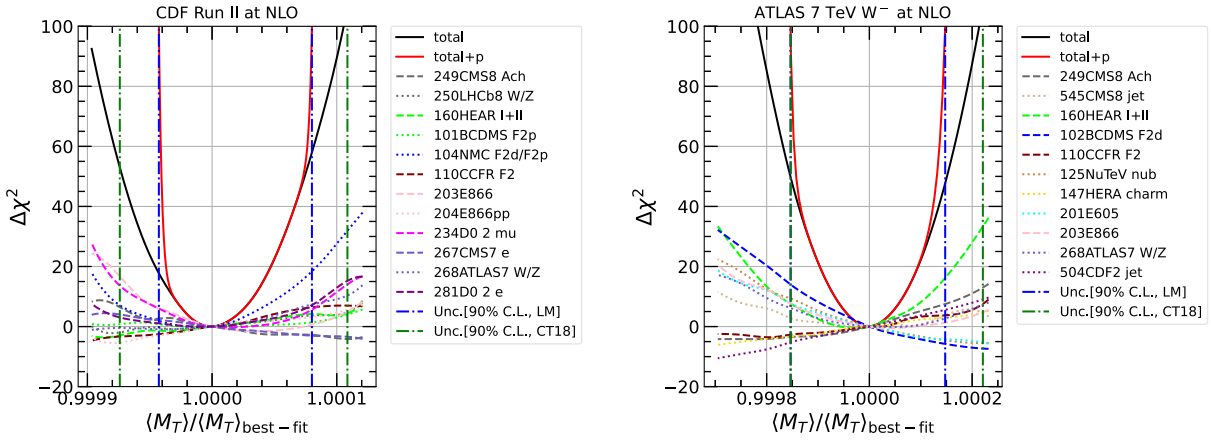

Fig. 7. (color online) LM scans on $\langle M_T\rangle$. The black and red solid lines represent $\Delta\chi^2$ and $\Delta\chi^2+P$, respectively. The dotted and dashed lines indicate the contributions to $\Delta\chi^2$ from individual data sets. The blue and green vertical dot-dashed lines represent the uncertainties at a 90% C.L. determined using the LM method and the Hessian method from the published CT18 NNLO PDFs, respectively.

the total constraints and cuts off the uncertainty range well before the global $\Delta\chi^2$ reaches the tolerance. The LM method gives a smaller PDF uncertainty than the estimation based on the Hessian method [124, 135]. In the case of W^- production at 7 TeV ATLAS, in the right panel, we find that BCDMS deuteron data along with HERA inclusive DIS data and 8 TeV CMS charge asymmetry data give the dominant constraints. In addition, the BCDMS deuteron data prefer a larger $\langle M_T\rangle$, which results in a large penalty term. The LM method again predicts a slightly smaller uncertainty than the Hessian method.

The contribution from an individual experimental data set can also be evaluated using LM scans with data subtracted. We remove one data set at a time and repeat the LM scans on $\langle M_T\rangle$ with the remaining data sets. The difference between the fit with and without the data set can be an assessment of its contribution. In Fig. 8, we show the results of LM scans on $\langle M_T\rangle$ with data subtracted. The results are normalized to the central value determined with full data sets. In the case of the CDF measurement, in the upper panel, we find that after the removal of most of the data set, the $\langle M_T\rangle$ value and its uncertainty only change slightly, as represented by the error bars, compared to the uncertainty from LM scans with full data sets, represented by the gray band. E866 Drell-Yan ratio data (Exp. ID = 203) along with D0 Run II charge asymmetry data (Exp. ID = 234) and NMC deuteron data (Exp. ID = 104) give strong constraints, which is consistent with the left panel of Fig. 7. In addition, we find that E866 Drell-Yan ratio data prefer a larger $\langle M_T\rangle$. In the case of $W^\pm$ production at 7 TeV ATLAS, in the lower panel, the constraints from HERA inclusive DIS data (Exp. ID = 160), E866 Drell-Yan ratio data (Exp. ID = 203), and 8 TeV CMS charge asymmetry data (Exp. ID = 249) predominate, as expected. After the inclusion of HERA inclusive DIS data or E866 Drell-Yan ratio data, the uncertainties of $\langle M_T\rangle$ are reduced by almost 50%. In addition, E866 Drell-Yan ratio data prefer a larger $\langle M_T\rangle$, in contrast with HERA inclusive DIS data and 8 TeV CMS charge asymmetry data, which prefer a smaller value.

C. Discussions

In the following, we perform a simple analysis to further understand the dependence of leptonic distributions on the PDFs, focusing on the p_T of the charged lepton in the CDF scenario. Note that at LO, p_T equals half of the transverse mass discussed earlier. We define θ^* as the polar angle between the decayed positron and anti-proton directions and y^* as the rapidity of the positron with respect to the proton direction, both in the rest frame of the W^+ boson. The following relations on kinematics hold at LO:

$$\cos\theta^* = -\tanh y^*,\ p_T = \frac{m_W}{2}\frac{1}{\cosh y^*}. \tag{10}$$

For the dominant partonic channel of $u\bar{d}$ annihilation, the LO partonic differential cross section with respect to $\cos\theta^*$ is proportional to $(1+\cos\theta^*)^2$ owing to the $V-A$ structure of the weak-charged current. This can be translated to

$$\frac{{\rm d}\hat{\sigma}}{{\rm d}y^*} \sim (1-\tanh y^*)^2/\cosh^2 y^*, \tag{11}$$

and a p_T weighted distribution,

$$p_T\frac{{\rm d}\hat{\sigma}}{{\rm d}y^*} \sim \frac{m_W}{2}(1-\tanh y^*)^2/\cosh^3 y^*. \tag{12}$$

From the above equations, we can calculate the mean

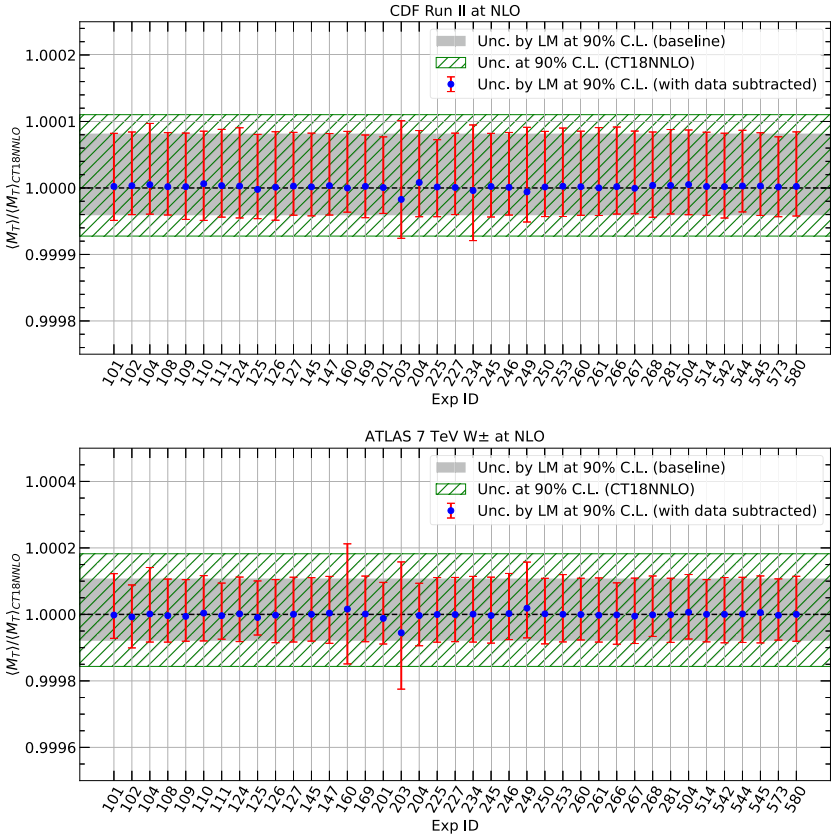

Fig. 8. (color online) Results of LM scans on $\langle M_T\rangle$ with data subtracted. The results are normalized to the central value determined with full data sets. The horizontal axis represents the experimental data set removed from the LM scans. The blue marks and red error bars indicate the central values and uncertainties at a 90% C.L., respectively, determined using the LM method with the remaining the data sets. The green hatched area and gray band represent the uncertainties at a 90% C.L., which are determined using the Hessian and LM methods with full data sets, respectively.

transverse momentum of the positron as $\frac{15\pi}{128}m_W \sim 0.368 m_W$. However, in the CDF analysis, the selection cut on the transverse momentum of the charged lepton imposes $|y^*| \lesssim 0.8$. Furthermore, if the W boson is boosted with a rapidity of y_b, the rapidity selection of the charged lepton also requires $|y^* + y_b| < 1$. Thus, the actual mean transverse momentum and acceptance of the charged lepton depend on y_b in a non-trivial way, as plotted in Fig. 9. We also show the distribution of y^* in Fig. 9, which peaks at a negative value because the positron is aligned with the $\bar{d}$ quark. The inequalities indicate the y^* region that contributes to the cross sections after selections for a fixed y_b. The mean transverse momentum peaks at a y_b value of approximately -0.8 because this excludes the peak region in y^*, which has a relatively smaller p_T. The mean transverse momentum decreases at large $|y_b|$ values because only high $|y^*|$ regions remain, which have low p_T. The acceptance is largest in the central region of y_b.

However, the transverse momentum distribution is a superposition of contributions from all possible rapidities of the W boson. The distribution of the latter is exactly determined by PDFs as

$$\frac{\mathrm{d}\sigma}{\mathrm{d}y_b} \sim f_{u/p}(x_1,\mu) f_{\bar{d}/\bar{p}}(x_2,\mu), \tag{13}$$

at LO for the $u\bar{d}$ partonic channel, with $x_{1,2} = m_W/\sqrt{s}\, e^{\pm y_b}$. The normalized rapidity distribution of the W boson based on the above equation is shown in Fig. 10 for a variety of PDFs, with the lepton acceptance shown in Fig. 9 applied. By combining Figs. 9 and 10, we can understand several features shown in Sec. IIA. For instance, by comparing the y_b distributions from the CT18, MSHT20, NNPDF3.1, and NNPDF4.0 NNLO PDFs, the ratios of NNPDF4.0 to others are shown to exhibit a clear positive slope across y_b. This leads to a reduction in the mean transverse momentum of the positron because it is, on average, smaller for $y_b > 0$, and also a reduction in the mean transverse mass of the leptons. The behavior of NNPDF4.0 can be traced back to the suppression of the d-quark PDF in the large-x region, in contrast with its previous generation, which suppresses the rapidity distribution in the anti-boost region. Similarly, the NLO PDFs

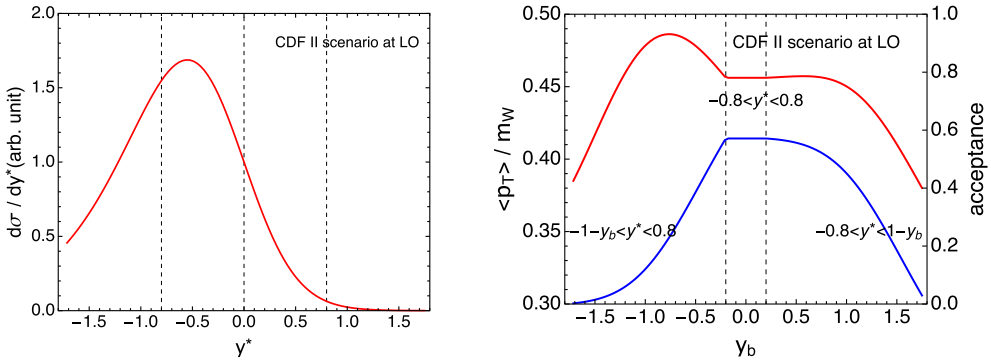

Fig. 9. (color online) Left: Rapidity distribution of the positron in the rest frame of the W^+ boson in the scenario of the CDF measurement calculated at LO for the $u\bar{d}$ partonic channel. Right: Mean transverse momentum (red with the scale on the left) and acceptance (blue with the scale on the right) of the positron after selections as a function of the rapidity of the W boson. The inequalities indicate the y^* region that contributes to the cross sections after selections for a fixed y_b.

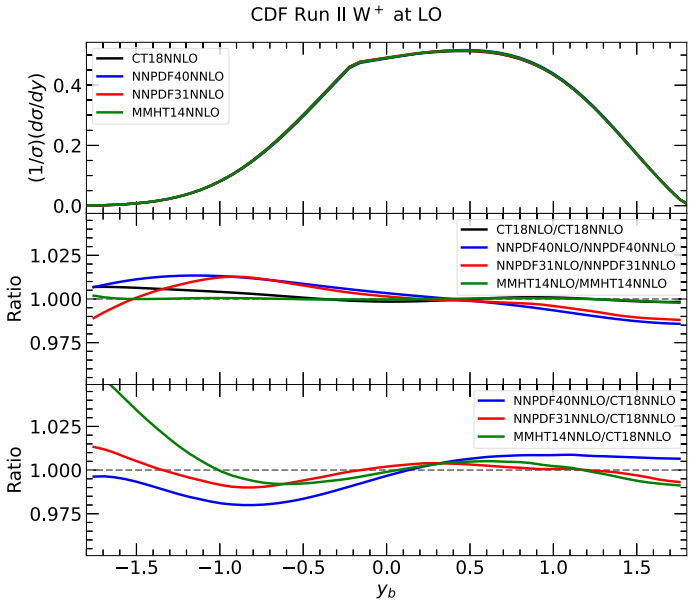

Fig. 10. (color online) Rapidity distribution of the W^+ boson at Tevatron Run II, calculated at LO and with lepton acceptance applied for the $u\bar{d}$ annihilation channel using a variety of NLO and NNLO PDFs.

give a larger mean transverse mass than NNLO PDFs in general, and the ratios of NLO to NNLO PDFs exhibit a negative slope in the middle panel of Fig. 10. However, this situation can change for different PDF groups because CT18 and MMHT14 present more stable predictions when using NLO PDFs than NNLO.

IV. SUMMARY

In summary, we study the dependence of the transverse mass distribution of charged leptons and the missing energy on PDFs, focusing on W boson mass measurements by the CDF and ATLAS collaborations. We compare the shape of the prediction distributions using various up-to-date PDFs. In particular, we compare the mean transverse mass adapted to each of the measurements. We find that the spread of predictions from different PDF sets can be significantly larger than the PDF uncertainty predicted by a specific PDF set. The mean transverse mass is strongly anti-correlated with the extracted W boson mass, as validated by the χ^2 fit and via a comparison with the experimental numbers of mass shift on PDF dependence. Thus, the analysis of experimental data using up-to-date PDFs could be highly desirable, especially considering tensions between different W boson mass measurements. We also examine theoretical uncertainties induced by factorization and renormalization scales, the strong coupling constant, and the W-boson decay width in the CDF context and find that the width dependence can be comparable if varied by an experimental error. Furthermore, we perform a series of LM scans to identify the constraints on the transverse mass distribution imposed by individual data sets in the CT18 global analysis of PDFs. In the

case of the CDF measurement, the distribution is mostly sensitive to d-quark PDFs in the intermediate x region, which are largely constrained by DIS and Drell-Yan data on deuteron targets as well as Tevatron lepton charge asymmetry data. For the ATLAS measurement, the strongest constraints arise from HERA inclusive DIS data, E866 Drell-Yan ratio data, and CMS lepton charge asymmetry data.

ACKNOWLEDGMENTS

We would like to thank Pavel Nadolsky, C.-P. Yuan, and other CTEQ-TEA collaborators for helpful discussions and comments. JG would like to thank Hong-Jian He for useful discussions. KX thanks PITT PACC colleagues for many stimulating discussions, particularly Tao Han for bringing up the W decay width effect.

References

[1] **CDF** Collaboration, T. Aaltonen *et al*., Science **376**(6589), 170-176 (2022)
[2] J. Haller, A. Hoecker, R. Kogler, K. Mönig, T. Peiffer, and J. Stelzer, Eur. Phys. J. C **78**(8), 675 (2018), arXiv:1803.01853[hep-ph]
[3] P. A. Zyla *et al*. (Particle Data Group), PTEP **2020**(8), 083C01 (2020)
[4] J. de Blas, M. Ciuchini, E. Franco *et al*., Phys. Rev. D **106**, 033003 (2022)
[5] C.-T. Lu, L. Wu, Y. Wu *et al*., Phys. Rev. D **106**, 035034 (2022)
[6] C.-R. Zhu, M.-Y. Cui, Z.-Q. Xia *et al*., *GeV antiproton/gamma-ray excesses and the W-boson mass anomaly: three faces of ~ 60 – 70 GeV dark matter particle?* arXiv: 2204.03767
[7] Y.-Z. Fan, T.-P. Tang, Y.-L. S. Tsai *et al*., *Inert Higgs Dark Matter for New CDF W-boson Mass and Detection Prospects*, arXiv: 2204.03693.
[8] A. Strumia, J. High Energ. Phys. **2022**, 248 (2022)
[9] J. M. Yang and Y. Zhang, Sci. Bull. **67**, 1430 (2022)
[10] T.-P. Tang, M. Abdughani, L. Feng *et al*., *NMSSM neutralino dark matter for W-boson mass and muon $g-2$ and the promising prospect of direct detection*, arXiv:2204.04356
[11] X. K. Du, Z. Li, F. Wang *et al*., *Explaining The Muon $g-2$ Anomaly and New CDF Ⅱ W-Boson Mass in the Framework of (Extra)Ordinary Gauge Mediation*, arXiv: 2204.04286
[12] C. Campagnari and M. Mulders, Science **376**(6589), abm0101 (2022)
[13] G. Cacciapaglia and F. Sannino, Phys. Lett. B **832**, 137232 (2022)
[14] M. Blennow, P. Coloma, E. Fernández-Martínez *et al*., *Right-handed neutrinos and the CDF Ⅱ anomaly*, arXiv:2204.04559
[15] K. Sakurai, F. Takahashi, and W. Yin, Phys. Lett. B **833**, 137324 (2022)
[16] B.-Y. Zhu, S. Li, J.-G. Cheng *et al*., *Using gamma-ray observation of dwarf spheroidal galaxy to test a dark matter model that can interpret the W-boson mass anomaly*, arXiv: 2204.04688
[17] F. Arias-Aragón, E. Fernández-Martínez, M. González-López *et al*., *Dynamical Minimal Flavour Violating Inverse Seesaw*, arXiv: 2204.04672
[18] X. Liu, S.-Y. Guo, B. Zhu *et al*., Sci. Bull. **67**, 1437 (2022)
[19] A. Paul and M. Valli, Phys. Rev. D **106**, 013008 (2022)
[20] K. S. Babu, S. Jana, and V.a P. K., Phys. Rev. Lett. **129**, 121803 (2022)
[21] J. Gu, Z. Liu, T. Ma *et al*., *Speculations on the W-Mass Measurement at CDF*, arXiv: 2204.05296
[22] L. Di Luzio, R. Gröber, and P. Paradisi, Phys. Lett. B **832**, 137250 (2022)
[23] J. J. Heckman, Phys. Lett. B **833**, 137387 (2022)
[24] H. M. Lee and K. Yamashita, Eur. Phys. J. C **82**, 661 (2022)
[25] Y. Cheng, X.-G. He, Z.-L. Huang *et al*., Phys. Lett. B **831**, 137218 (2022)
[26] H. Bahl, J. Braathen, and G. Weiglein, Phys. Lett. B **833**, 137295 (2022)
[27] H. Song, W. Su, and M. Zhang, *Electroweak Phase Transition in 2HDM under Higgs, Z-pole, and W precision measurements*, arXiv: 2204.05085
[28] P. Asadi, C. Cesarotti, K. Fraser *et al*., *Oblique Lessons from the W Mass Measurement at CDF Ⅱ*, arXiv: 2204.05283
[29] P. Athron, M. Bach, D. H. J. Jacob *et al*., *Precise calculation of the W boson pole mass beyond the Standard Model with FlexibleSUSY*, arXiv: 2204.05285
[30] Y. Heo, D.-W. Jung, and J. S. Lee, Phys. Lett. B **833**, 137274 (2022)
[31] A. Crivellin, M. Kirk, T. Kitahara *et al*., Phys. Rev. D **106**, L031704 (2022)
[32] M. Endo and S. Mishima, *New physics interpretation of W-boson mass anomaly*, arXiv: 2204.05965
[33] X. K. Du, Z. Li, F. Wang *et al*., *Explaining The New CDF Ⅱ W-Boson Mass Data In The Georgi-Machacek Extension Models*, arXiv: 2204.05760
[34] K. Cheung, W.-Y. Keung, and P.-Y. Tseng, Phys. Rev. D **106**, 015029 (2022)
[35] L. Di Luzio, M. Nardecchia, and C. Toni, Phys. Rev. D **105**, 115042 (2022)
[36] T. Biekötter, S. Heinemeyer, and G. Weiglein, *Excesses in the low-mass Higgs-boson search and the W-boson mass measurement*, arXiv: 2204.05975
[37] N. V. Krasnikov, *Nonlocal generalization of the SM as an explanation of recent CDF result*, arXiv: 2204.06327
[38] M.-D. Zheng, F.-Z. Chen, and H.-H. Zhang, *The $W\ell\nu$-vertex corrections to W-boson mass in the R-parity violating MSSM*, arXiv: 2204.06541
[39] Y. H. Ahn, S. K. Kang, and R. Ramos, *Implications of New CDF-Ⅱ W Boson Mass on Two Higgs Doublet Model*, arXiv: 2204.06485
[40] K.-S. Sun, W.-H. Zhang, J.-B. Chen *et al*., *The lepton flavor violating decays of vector mesons in the MRSSM*, arXiv: 2204.06234
[41] J. Kawamura, S. Okawa, and Y. Omura, Phys. Rev. D **106**, 015005 (2022)
[42] Z. Péli and Z. Trócsányi, *Vacuum stability and scalar masses in the superweak extension of the standard model*, arXiv: 2204.07100

[43] A. Ghoshal, N. Okada, S. Okada *et al.*, *Type III seesaw with R-parity violation in light of m_W (CDF)*, arXiv: 2204.07138

[44] P. Fileviez Perez, H. H. Patel, and A. D. Plascencia, Phys. Lett. B **833**, 137371 (2022)

[45] K. I. Nagao, T. Nomura, and H. Okada, *A model explaining the new CDF II W boson mass linking to muon $g-2$ and dark matter*, arXiv: 2204.07411

[46] S. Kanemura and K. Yagyu, Phys. Lett. B **831**, 137217 (2022)

[47] P. Mondal, Phys. Lett. B **833**, 137357 (2022)

[48] R. A. Wilson, A toy model for the W/Z mass ratio, arXiv: 2204.07970

[49] K.-Y. Zhang and W.-Z. Feng, *Explaining W boson mass anomaly and dark matter with a $U(1)$ dark sector*, arXiv: 2204.08067

[50] V. Cirigliano, W. Dekens, J. de Vries *et al.*, *Beta-decay implications for the W-boson mass anomaly*, arXiv: 2204.08440

[51] D. Borah, S. Mahapatra, D. Nanda *et al.*, Phys. Lett. B **833**, 137297 (2022)

[52] T. A. Chowdhury, J. Heeck, S. Saad *et al.*, Phys. Rev. D **106**, 035004 (2022)

[53] G. Arcadi and A. Djouadi, *The 2HD+a model for a combined explanation of the possible excesses in the CDF* $\mathbf{M_W}$ measurement and $(g-2)_\mu$ *with Dark Matter*, arXiv: 2204.08406

[54] O. Popov and R. Srivastava, *The Triplet Dirac Seesaw in the View of the Recent CDF-II W Mass Anomaly*, arXiv: 2204.08568

[55] L. M. Carpenter, T. Murphy, and M. J. Smylie, Phys. Rev. D **106**, 055005 (2022)

[56] A. Bhaskar, A. A. Madathil, T. Mandal *et al.*, *Combined explanation of W-mass, muon $g-2$, $R_{K^{(*)}}$ and $R_{D^{(*)}}$ anomalies in a singlet-triplet scalar leptoquark model*, arXiv: 2204.09031

[57] K. Ghorbani and P. Ghorbani, *W-Boson Mass Anomaly from Scale Invariant 2HDM*, arXiv: 2204.09001

[58] M. Du, Z. Liu, and P. Nath, Phys. Lett. B **834**, 137454 (2022)

[59] Y.-P. Zeng, C. Cai, Y.-H. Su *et al.*, *Extra boson mix with Z boson explaining the mass of W boson*, arXiv: 2204.09487

[60] A. Batra, S. K. A., S. Mandal *et al.*, *W boson mass in Singlet-Triplet Scotogenic dark matter model*, arXiv: 2204.09376

[61] D. Borah, S. Mahapatra, and N. Sahu, Phys. Lett. B **831**, 137196 (2022)

[62] J. Cao, L. Meng, L. Shang *et al.*, *Interpreting the W mass anomaly in the vectorlike quark models*, arXiv: 2204.09477

[63] S. Baek, *Implications of CDF W-mass and $(g-2)_\mu$ on $U(1)_{L_\mu-L_\tau}$ model*, arXiv: 2204.09585

[64] J. Heeck, *W-boson mass in the triplet seesaw model*, arXiv: 2204.10274

[65] A. Addazi, A. Marciano, A. P. Morais *et al.*, *CDF II W-mass anomaly faces first-order electroweak phase transition*, arXiv: 2204.10315

[66] Y. Cheng, X.-G. He, F. Huang *et al.*, Phys. Rev. D **106**, 055011 (2022)

[67] E. d. S. Almeida, A. Alves, O. J. P. Eboli *et al.*, *Impact of CDF-II measurement of M_W on the electroweak legacy of the LHC Run II*, arXiv: 2204.10130

[68] S. Lee, K. Cheung, J. Kim *et al.*, *Status of the two-Higgs-doublet model in light of the CDF m_W measurement*, arXiv: 2204.10338

[69] C. Cai, D. Qiu, Y.-L. Tang *et al.*, *Corrections to electroweak precision observables from mixings of an exotic vector boson in light of the CDF W-mass anomaly*, arXiv: 2204.11570

[70] R. Benbrik, M. Boukidi, and B. Manaut, *W-mass and 96 GeV excess in type-III 2HDM*, arXiv: 2204.11755

[71] T. Yang, S. Qian, S. Deng *et al.*, *The physics case for a neutrino lepton collider in light of the CDF W mass measurement*, arXiv: 2204.11871

[72] A. Batra, S. K. A, S. Mandal *et al.*, *CDF-II W Boson Mass Anomaly in the Canonical Scotogenic Neutrino-Dark Matter Model*, arXiv: 2204.11945

[73] A. E. Faraggi and M. Guzzi, *Z's and sterile neutrinos from heterotic string models: exploring Z' mass exclusion limits*, arXiv: 2204.11974

[74] H. B. T. Tan and A. Derevianko, *Implications of W-boson mass anomaly for atomic parity violation*, arXiv: 2204.11991

[75] H. Abouabid, A. Arhrib, R. Benbrik *et al.*, *Is the new CDF M_W measurement consistent with the two higgs doublet model?* arXiv: 2204.12018

[76] R. Rahaman, *On two-body and three-body spin correlations in leptonic $t\bar{t}Z$ production and anomalous couplings at the LHC*, arXiv: 2204.12152

[77] T.-K. Chen, C.-W. Chiang, and K. Yagyu, Phys. Rev. D **106**, 055035 (2022)

[78] R. Dermisek, J. Kawamura, E. Lunghi *et al.*, *Leptonic cascade decays of a heavy Higgs boson through vectorlike leptons at the LHC*, arXiv: 2204.13272

[79] R. S. Gupta, *Running away from the T-parameter solution to the W mass anomaly*, arXiv: 2204.13690

[80] V. Basiouris and G. K. Leontaris, *Sterile neutrinos, $0\nu\beta\beta$ decay and the W-boson mass anomaly in a Flipped $SU(5)$ from F-theory*, arXiv: 2205.00758

[81] J.-W. Wang, X.-J. Bi, P.-F. Yin *et al.*, Phys. Rev. D **106**, 055001 (2022), arXiv:2205.00783 [hep-ph]

[82] F. J. Botella, F. Cornet-Gomez, C. Miró *et al.*, *Muon and electron $g-2$ anomalies in a flavor conserving 2HDM with an oblique view on the CDF M_W value*, arXiv: 2205.01115

[83] J. Kim, Phys. Lett. B **832**, 137220 (2022)

[84] J. Kim, S. Lee, P. Sanyal *et al.*, Phys. Rev. D **106**, 035002 (2022)

[85] B. Barman, A. Das, and S. Sengupta, *New W-Boson mass in the light of doubly warped braneworld model*, arXiv: 2205.01699

[86] S.-P. He, *A leptoquark and vector-like quark extended model for the simultaneous explanation of the W boson mass and muon $g-2$* anomalies, arXiv: 2205.02088

[87] X.-Q. Li, Z.-J. Xie, Y.-D. Yang *et al.*, *Correlating the CDF W-boson mass shift with the $b\to s\ell^+\ell^-$ anomalies*, arXiv: 2205.02205

[88] R. Dcruz and A. Thapa, *W boson mass, dark matter and $(g-2)_\ell$ in ScotoZee neutrino mass model*, arXiv: 2205.02217

[89] A. W. Thomas and X. G. Wang, Phys. Rev. D **106**, 056017 (2022)

[90] X.-F. Han, F. Wang, L. Wang *et al.*, Chin. Phys. C **46**, 103105 (2022)

[91] Q. Zhou and X.-F. Han, *The CDF W-mass, muon g-2, and dark matter in a $U(1)_{L_\mu-L_\tau}$ model with vector-like leptons*,

" arXiv: 2204.13027
[92] J. de Blas, M. Pierini, L. Reina *et al*., *Impact of the recent measurements of the top-quark and W-boson masses on electroweak precision fits*, arXiv: 2204.04204
[93] J. Fan, L. Li, T. Liu *et al*., *W-Boson Mass, Electroweak Precision Tests and SMEFT*, arXiv: 2201.06586
[94] E. Bagnaschi, J. Ellis, M. Madigan *et al*., *SMEFT Analysis of* m_W, arXiv: 2204.05260
[95] R. Balkin, E. Madge, T. Menzo *et al*., *On the implications of positive W mass shift*, arXiv: 2204.05992
[96] P. Athron, A. Fowlie, C.-T. Lu *et al*., *The W boson Mass and Muon* $g-2$*: Hadronic Uncertainties or New Physics?* arXiv: 2204.03996
[97] M. Pellen, R. Poncelet, A. Popescu *et al*., *Angular coefficients in W+j production at the LHC with high precision*, arXiv: 2204.12394
[98] L.-B. Chen, L. Dong, H. T. Li *et al*., *One-loop squared amplitudes for hadronic tW production at next-to-next-to-leading order in QCD*, arXiv: 2204.13500
[99] Z. Liu and L.-T. Wang, *Physics at Future Colliders: the Interplay Between Energy and Luminosity*, *in 2022 Snowmass Summer Study*. 4, 2022. arXiv: 2205.00031
[100] J. Isaacson, Y. Fu, and C. P. Yuan, *ResBos2 and the CDF W Mass Measurement*, arXiv: 2205.02788
[101] M. Aaboud *et al*. (ATLAS Collaboration), Eur. Phys. J. C **78**(2), 110 (2018), arXiv:1701.07240[hep-ex].[Erratum:Eur.Phys.J.C78,898(2018)]
[102] R. Aaij *et al*. (LHCb Collaboration), JHEP **01**, 036 (2022), arXiv:2109.01113[hep-ex]
[103] T. A. Aaltonen *et al*. (CDF and D0 Collaborations), Phys. Rev. D **88**(5), 052018 (2013), arXiv:1307.7627[hep-ex]
[104] S. Schael *et al*. (ALEPH, DELPHI, L3, OPAL Collaborations, and LEP Electroweak Working Group), Phys. Rept. **532**, 119-244 (2013), arXiv:1302.3415[hep-ex]
[105] R. D. Ball *et al*. (NNPDF Collaboration), Eur. Phys. J. C **77**(10), 663 (2017), arXiv:1706.00428[hep-ph]
[106] J. Gao, M. Guzzi, J. Huston *et al*., Phys. Rev. D **89**(3), 033009 (2014), arXiv:1302.6246[hep-ph]
[107] T.-J. Hou *et al*., Phys. Rev. D **103**(1), 014013 (2021), arXiv:1912.10053[hep-ph]
[108] S. Bailey, T. Cridge, L. A. Harland-Lang *et al*., Eur. Phys. J. C **81**(4), 341 (2021), arXiv:2012.04684[hep-ph]
[109] P. M. Nadolsky, AIP Conf. Proc. **753**(1), 158-170 (2005), arXiv:hep-ph/0412146
[110] G. Bozzi, L. Citelli, and A. Vicini, Phys. Rev. D **91**(11), 113005 (2015), arXiv:1501.05587[hep-ph]
[111] S. Farry, O. Lupton, M. Pili *et al*., Eur. Phys. J. C **79**(6), 497 (2019), arXiv:1902.04323[hep-ex]
[112] E. Bagnaschi and A. Vicini, Phys. Rev. Lett. **126**(4), 041801 (2021), arXiv:1910.04726[hep-ph]
[113] M. Hussein, J. Isaacson, and J. Huston, J. Phys. G **46**(9), 095002 (2019), arXiv:1905.00110[hep-ph]
[114] J. M. Campbell and R. K. Ellis, Phys. Rev. D **60**, 113006 (1999), arXiv:hep-ph/9905386
[115] J. M. Campbell, R. K. Ellis, and C. Williams, JHEP **07**, 018 (2011), arXiv:1105.0020[hep-ph]
[116] T. Carli, D. Clements, A. Cooper-Sarkar *et al*., Eur. Phys. J. C **66**, 503-524 (2010), arXiv:0911.2985[hep-ph]
[117] D. Stump, J. Huston, J. Pumplin *et al*., JHEP **10**, 046 (2003), arXiv:hep-ph/0303013
[118] L. A. Harland-Lang, A. D. Martin, P. Motylinski *et al*., Eur. Phys. J. C **75**(5), 204 (2015), arXiv:1412.3989[hep-ph]
[119] R. D. Ball *et al*., *The Path to Proton Structure at One-Percent Accuracy*, arXiv: 2109.02653
[120] J. Gao, L. Harland-Lang, and J. Rojo, Phys. Rept. **742**, 1-121 (2018), arXiv:1709.04922[hep-ph]
[121] W.-K. Tung, S. Kretzer, and C. Schmidt, J. Phys. G **28**, 983-996 (2002), arXiv:hep-ph/0110247
[122] Kotwal, Ashutosh V, Phys. Rev. D **98**(3), 033008 (2018)
[123] S. Dulat, T.-J. Hou, J. Gao, *et al*., Phys. Rev. D **93**(3), 033006 (2016), arXiv:1506.07443[hep-ph]
[124] A. D. Martin, W. J. Stirling, R. S. Thorne *et al*., Eur. Phys. J. C **63**, 189-285 (2009), arXiv:0901.0002[hep-ph]
[125] R. D. Ball *et al*., Nucl. Phys. B **867**, 244-289 (2013), arXiv:1207.1303[hep-ph]
[126] S. Alekhin, J. Blümlein, S. Moch *et al*., Phys. Rev. D **96**(1), 014011 (2017), arXiv:1701.05838[hep-ph]
[127] H. Abramowicz *et al*. (H1and ZEUS Collaborations), Eur. Phys. J. C **75**(12), 580 (2015), arXiv:1506.06042[hep-ex]
[128] G. Aad *et al*. (ATLAS Collaboration), JHEP **07**, 223 (2021), arXiv:2101.05095[hep-ex]
[129] A. Accardi, L. T. Brady, W. Melnitchouk *et al*., Phys. Rev. D **93**(11), 114017 (2016), arXiv:1602.03154[hep-ph]
[130] Tevatron Electroweak Working Group, *Combination of CDF and D0 Results on the Width of the W boson*, arXiv: 1003.2826
[131] J. Gao and P. Nadolsky, JHEP **07**, 035 (2014), arXiv:1401.0013[hep-ph]
[132] J. Pumplin, D. R. Stump, and W. K. Tung, Phys. Rev. D **65**, 014011 (2001), arXiv:hep-ph/0008191
[133] D. Stump, J. Pumplin, R. Brock *et al*., Phys. Rev. D **65**, 014012 (2001), arXiv:hep-ph/0101051
[134] D. Liu, C. Sun, and J. Gao, *Machine learning of log-likelihood functions in global analysis of parton distributions*, arXiv: 2201.06586
[135] J. Pumplin, D. Stump, R. Brock *et al*., Phys. Rev. D **65**, 014013 (2001), arXiv:hep-ph/0101032